A Brownian motor with real-time external steering and induced drifts along pre-designed paths
Supplementary Material

H. Hagman,[1] M. Zelan,[1] C. M. Dion,[1] A. Kastberg,[2]

[1]Department of Physics, Umeå University, SE-90187 Umeå, Sweden,
[2]Laboratoire de Physique de la Matière Condensée, CNRS UMR 6622,
Université de Nice-Sophia Antipolis, Parc Valrose, 06108 Nice Cedex 2, France

Materials and Methods

Detailed descriptions of the general experimental setup are given in (*1–3*). More details concerning the construction and the control of the Brownian motor are found in (*3–5*). In short, cesium atoms are first accumulated in a magneto-optical trap (*6–9*), from where they are transferred to the double optical lattice (*1*). Both lattices have a 3D topography and are constructed from a four beam configuration, in which two beams are propagating in the xz-plane, and two in yz-plane. All beams have a 45° angle with respect to the vertical z-axis with polarizations perpendicular to the plane of propagation ("3D lin⊥lin configuration" (*10*)).

The optical lattices are state-dependent and operate from different hyperfine ground states within the Cs D2 line, $6\mathrm{s}\,^2\mathrm{S}_{1/2} \rightarrow 6\mathrm{p}\,^2\mathrm{P}_{3/2}$ (*11*). Lattice S operates close to the $F_\mathrm{g} = 3 \rightarrow F_\mathrm{e} = 4$ transition and lattice L operates close to the $F_\mathrm{g} = 4 \rightarrow F_\mathrm{e} = 5$ transition. The detuning from atomic resonance where kept around 15Γ in lattice S and 35Γ in lattice L, where Γ is the natural linewidth of the excited state. This near-resonance makes incoherent light scattering important, including optical pumping within the manifold of Zeeman substates for a given ground state F_g, and results in diffusion within each lattice even tough the potential depths are significantly larger then the average kinetic energy of the atoms. Moreover, the optical lattices are dissipative, that is, an effective friction is present due to Sisyphus cooling (*6–8*). The results presented are taken for potential depths around $1000E_\mathrm{r}$ in lattice S and $2000E_\mathrm{r}$ in lattice L, where E_r is the recoil energy, while the typical root-mean-squared atomic velocity is of the order of $10v_\mathrm{r}$, where v_r is the recoil velocity (*11, 12*). The latter corresponds to a kinetic temperature around 10 μK, with potential depths around 100 μK in lattice S and 200 μK in lattice L.

The incoherent light scattering also provides a route between the two optical lattices, via a manifold of short-lived excited states. Since one of the lattices is based on a open transition ($F_\mathrm{g} = 3 \rightarrow F_\mathrm{e} = 4$), and the other on a closed transition ($F_\mathrm{g} = 4 \rightarrow F_\mathrm{e} = 5$), the transfer rates between them will be highly unequal (*1*), which generates one short-lived and one long-lived optical lattice (denoted S and L, respectively). The relative size of the transfer rates depends on the parameter settings of the lattices, but typically the atoms spend around 90% of their time in lattice L (*2*).

The optical lattice configuration consists of four arms, each with two laser beams (one for each optical lattice) of slightly different wavelengths with orthogonal polarizations. In each arm an electro-optical phase modulators (EOM) is placed, which controls the relative phase between the two beams through an applied voltage over the crystal inside the EOM. These crystals have one electro-optical active axis and one passive axis. Along the active axis the index of refraction is dependent on the applied voltage, modifying the optical path length, while the latter remains unchanged along the passive axis. After the EOMs, but before the different arms start to overlap, the polarizations of the two beams in each arm are turned to the same direction. When the four beams overlap, the resulting interference pattern creates a position-dependent potential for each Zeeman substate for a given ground state (*10*).

Since the two optical lattices are build with lasers of different wavelength, their spatial periodicity differs slightly. However, a complete dephasing of the two lattices due to this difference occurs on a scale of the order of centimeters, while the size of the optical lattices in the experiment is of the order of millimeters. For our purposes, we can therefore consider the periodicities of the two lattices to be equal.

The dependence of the induced drift on the relative phase in one dimension is close to sinusoidal, with a flattening for small phases, see figure S1A. The shape of the curves depends slightly on the chosen parameters, but the maximum drift occurs around $\varphi = 2\pi/3$. The relative phase settings for inducing drifts in other directions than along the Cartesian axes is non-trivial, due to a dimensional coupling in the system (*13*). In addition, the kinetic temperature of the

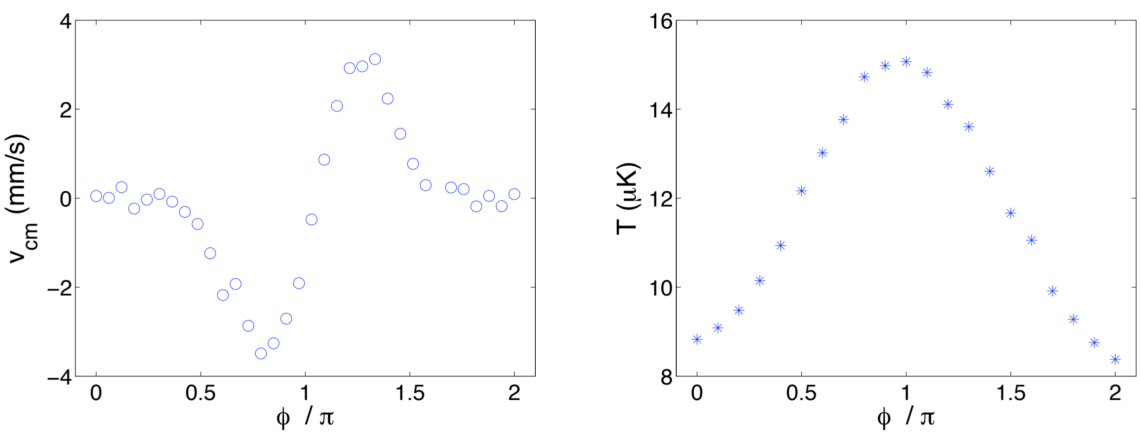

Figure S1: (A) Induced average velocity versus relative phase of the potentials. (B) Kinetic temperature versus relative phase of the potentials.

atoms is dependent on the relative phase between the lattices (*2*). This dependence is close to perfectly sinusoidal in our system, with a minimum for $\varphi = 0$, see figure S1B, and is used to ensure that the correct relative phases are applied (*14, 15*). To measure the temperature of the atomic cloud a time-of-flight technique is used (*14*). This detection technique is destructive, that is, for each measurement all atoms are lost from the interaction region. To follow the evolution of the same atoms is therefore impossible, and data presented with this detection technique are the result of several repetitions of the experiment, with a stepwise increase in interaction time (figure 2C) or relative phase (figure S1).

For this experiment, a non-invasive detection system has been realized. The incoherent light scattering gives the atoms in the optical lattices an inherent fluorescence, which we detect with an infrared-sensitive camera. The detection does therefore not interfere with the system and, unlike time-of-flight detection or absorption imaging, the same atoms can therefore be continuously monitored. With the current camera, images of the atomic cloud are extracted with a rate of 25 frames/sec. These images are saved and analyzed by the control system, extracting the center of mass position and the size of the atomic cloud. This analysis could be done in real time, and hence a feedback system could be realized.

As mentioned in the main text, in addition to the relative phase shift between the lattices, an additional difference between the two lattices is needed to break the spatio-temporal symmetry. In our case, we consider that the unequal transfer rates between the lattices is the main component of the symmetry breaking. In principle, any parameter characterizing the optical lattices (*e.g.*, potential depth) can be used to break the symmetry, by setting unequal values for the two lattices.

References

1. H. Ellmann, J. Jersblad, A. Kastberg, *Phys. Rev. Lett.* **90**, 053001 (2003).

2. H. Ellmann, J. Jersblad, A. Kastberg, *Eur. Phys. J. D* **22**, 355 (2003).

3. S. J. H. Petra, P. Sjölund, A. Kastberg, *J. Opt. A: Pure Appl. Opt.* **8**, 381 (2006).

4. P. Sjölund, *et al.*, *Phys. Rev. Lett.* **96**, 190602 (2006).

5. P. Sjölund, *et al.*, *Eur. Phys. J. D* **44**, 381 (2007).

6. W. D. Phillips, *Rev. Mod. Phys.* **70**, 721 (1998).

7. S. Chu, *Rev. Mod. Phys.* **70**, 685 (1998).

8. C. N. Cohen-Tannoudji, *Rev. Mod. Phys.* **70**, 707 (1998).

9. H. J. Metcalf, P. van der Straten, *J. Opt. Soc. Am. B* **20**, 887 (2003).

10. G. Grynberg, C. Robilliard, *Phys. Rep.* **355**, 335 (2001).

11. D. A. Steck, Cesium D line data, *Tech. Rep. LA-UR-03-7943*, Los Alamos National Laboratory (2003). Http://steck.us/alkalidata/.

12. The recoil velocity v_r corresponds to the change in velocity of the atom due to the recoil from the emission of one photon, and the recoil energy $E_\mathrm{r} \equiv m v_\mathrm{r}^2/2$, with m the mass of the atom.

13. H. Hagman, C. M. Dion, P. Sjölund, S. J. H. Petra, A. Kastberg, *EPL* **81**, 33001 (2008).

14. H. Hagman, *et al.*, *J. Appl. Phys.* **105**, 083109 (2009).

15. H. Ellmann, J. Jersblad, A. Kastberg, *Phys. Rev. Lett.* **90**, 053001 (2003).